

# Fabrication of uniform Ag/TiO<sub>2</sub> nanotube array structures with enhanced photoelectrochemical performance

Yuekun Lai,<sup>ab</sup> Huifang Zhuang,<sup>a</sup> Kunpeng Xie,<sup>a</sup> Dangguo Gong,<sup>b</sup> Yuxin Tang,<sup>b</sup> Lan Sun,<sup>a</sup> Changjian Lin<sup>\*a</sup> and Zhong Chen<sup>\*b</sup>

Received (in Montpellier, France) 23rd December 2009, Accepted 18th February 2010

First published as an Advance Article on the web 7th April 2010

DOI: 10.1039/b9nj00780f

In the current work, pulse current deposition has been used to prepare evenly distributed and uniformly sized Ag nanoparticles on a TiO<sub>2</sub> nanotube array photoelectrode. The Ag particle size and loading were controlled by the pulse deposition time. The Ag/TiO<sub>2</sub> nanotube arrays were characterized by SEM, TEM, XRD, XPS and UV-vis diffuse reflection absorption. The resulting electrode contained intimately coupled, three-dimensional Ag/TiO<sub>2</sub> structures with greatly improved photocurrent generation and charge transfer compared to a two-dimensional random Ag particle layer deposited directly on top of the nanotube array by the regular photoinduction method. A model mechanism is proposed to illustrate the uniform Ag nanoparticle deposition *via* the new deposition technique developed in the current work that promotes the uniform distribution of the Ag particles whilst minimizing their deposition at tube entrances, thus effectively preventing the pores from becoming clogged.

## 1. Introduction

In recent years, one-dimensional TiO<sub>2</sub> array nanostructures, especially self-organized TiO<sub>2</sub> nanotube arrays prepared by electrochemical anodizing, have attracted much attention<sup>1–3</sup> for applications in photovoltaic cells,<sup>4–6</sup> environmental purification,<sup>7–9</sup> water photolysis,<sup>10,11</sup> wettability control,<sup>12,13</sup> gas sensors<sup>14,15</sup> and biomedical devices<sup>16,17</sup> due to their unique highly ordered array structure, good mechanical and chemical stability, excellent corrosion resistance and high specific surface area. However, their photocatalytic efficiency is limited because of low visible light utilization and the high recombination rate of photogenerated electron–hole pairs. Many groups have since attempted to improve the light absorption efficiency by various approaches, including transition metal cation doping,<sup>18,19</sup> non-metal anion doping,<sup>20–22</sup> semiconductor heterojunctions<sup>23–25</sup> and surface modification with noble metals.<sup>26–31</sup> These purposes are to increase the light sensitivity range and suppress the recombination of photogenerated electron–hole pairs. In terms of the modified noble metal, Ag is one of the most suitable candidates for industrial applications due to its low cost and ease of preparation. To the best of our knowledge, photoinduced deposition and calcination reduction are the only two main methods employed to deposit Ag nanoparticles onto TiO<sub>2</sub> photocatalysts.<sup>28–31</sup> However, neither approach is able to prevent the aggregation of Ag particles and keep structures uniform during the deposition process.

To avoid the problem of particle aggregation and further enhance the photoelectrochemical activity, we have developed

a simple method using pulse current (PC) deposition to deposit small and uniformly distributed spherical Ag nanoparticles onto the surface of prepared TiO<sub>2</sub> nanotube arrays. This process is easy to implement and can effectively suppress the agglomeration of Ag particles by taking advantage of the high nucleation rate under the PC. The experimental results indicate that the Ag-decorated photocatalysts prepared by the PC process show a great enhancement of the photoelectrochemical activity compared to Ag/TiO<sub>2</sub> electrodes prepared by photoreduction. Finally, the formation mechanism is discussed for uniformly dispersed Ag particles on the surface of TiO<sub>2</sub> nanotube arrays.

## 2. Experimental

### 2.1 Preparation of TiO<sub>2</sub> nanotube array films

99.6% purity titanium foils, 0.1 mm thick, were used in the experiments to prepare TiO<sub>2</sub> nanotube structures by anodization. Prior to anodization, the titanium foils (10 × 10 mm<sup>2</sup>) were de-greased in an ultrasonic bath in acetone, anhydrous ethanol and de-ionized (DI) water successively, followed by rinsing with DI water and drying in air. TiO<sub>2</sub> nanotube array layers were fabricated in 0.5 wt% HF electrolyte using the previously reported electrochemical anodizing technique.<sup>32,33</sup> Non-porous TiO<sub>2</sub> layers were also fabricated as a reference sample by anodizing Ti in 1M H<sub>2</sub>SO<sub>4</sub> at 20 V for 20 min. The as-anodized amorphous TiO<sub>2</sub> nanotubes were subsequently annealed at 450 °C in air for 2 h and then cooled at 5 °C min<sup>-1</sup> to induce the formation of crystalline anatase.

### 2.2 Pulse current electrodeposition of Ag nanoparticles

PC deposition was carried out in an aqueous solution of 10 mM AgNO<sub>3</sub> and 100 mM NaNO<sub>3</sub> at room temperature. The TiO<sub>2</sub> nanotube substrate (10 × 10 mm<sup>2</sup>) and Pt plate

<sup>a</sup> State Key Laboratory of Physical Chemistry of Solid Surfaces, and College of Chemistry and Chemical Engineering, Xiamen University, Xiamen 361005, China. E-mail: cjlin@xmu.edu.cn

<sup>b</sup> School of Materials Science and Engineering, Nanyang Technological University, 50 Nanyang Avenue, Singapore 639798, Singapore. E-mail: aszchen@ntu.edu.sg

( $20 \times 20 \text{ mm}^2$ ) were used as the working and counter electrodes, respectively. A PC of  $10 \text{ mA cm}^{-2}$  with an alternating 0.1 s on-time and 0.3 s off-time was controlled by an Autolab PGSTAT30 Potentiostat/Galvanostat. To compare the morphology and performance of the Ag/TiO<sub>2</sub> electrodes, the conventional photoreduction method was also carried out by soaking the TiO<sub>2</sub> electrodes in a 10 mM AgNO<sub>3</sub> and 0.1 M methanol solution with or without ultrasonication, followed by irradiation with a 20 W UV lamp.

### 2.3 Materials characterizations

The structure and morphology of the TiO<sub>2</sub> nanotube array electrode loaded with pulse-deposited and photoreduced Ag nanoparticles were observed under a scanning electron microscope (SEM, LEO-1530) and by transmission electron microscopy (TEM, Tecnai-F30). The crystal structure of the Ag-modified TiO<sub>2</sub> nanotube arrays were analyzed with an X-ray diffractometer (Philips, Panalytical X'pert, Cu-K<sub>α</sub> radiation). The chemical composition of the TiO<sub>2</sub> nanotubes was characterized by X-ray photoelectron spectroscopy (XPS, VG 2000) using Al-K<sub>α</sub> monochromated radiation as the exciting source. The binding energy of the target element (Ag) was determined by using the binding energy of carbon (C 1s: 284.8 eV) as a reference. The absorption properties of the nanotube array samples were investigated using a diffuse reflectance UV-vis spectrometer (Varian, Cary 5000) with wavelengths in the 300–500 nm range.

### 2.4 Photoelectrochemical performance measurements

Electrochemical impedance spectroscopy (EIS) was recorded by applying an AC voltage of 10 mV amplitude over the frequency range 0.01 Hz to 100 kHz in a 0.1 M Na<sub>2</sub>SO<sub>4</sub> solution. The photoelectrochemical measurements were carried out in an electrochemical cell with a quartz window, where the as-prepared Ag/TiO<sub>2</sub> nanostructured film served as the working electrode and a platinum wire was used as the counter electrode in a supporting electrolyte of 0.1 M Na<sub>2</sub>SO<sub>4</sub> aqueous solution. A 150 W Xe lamp with a monochromator was used as the light source. The generated photocurrent signal was collected using a lock-in amplifier synchronized with a light chopper. All measurements were controlled and recorded by a microcomputer under zero bias in the range 250–600 nm.

## 3. Results and discussion

### 3.1 Scheme of PC deposition

Fig. 1 shows a diagram of the electrodeposition process with a rectangular pulse shape. The PC process comprises a series of alternating pulse-on ( $T_{\text{on}} = 0.1 \text{ s}$ ) and pulse-off ( $T_{\text{off}} = 0.3 \text{ s}$ ) events. Compared with conventional direct current deposition, the longer off-time (or relaxation period) in the PC process allows time for the depleted metal ions to replenish near the substrate surface, enhancing the nucleation rate and depressing dendritic growth.<sup>34,35</sup> Therefore, the current technique makes it easy to prepare a uniform Ag film with a controlled particle size. Moreover, the size and density of Ag particles can be controlled by varying the current density and the on/off times.

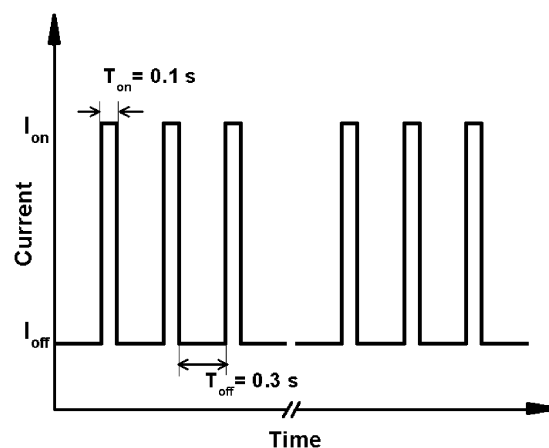


Fig. 1 A diagram of the PC process with a rectangular pulse shape.  $T_{\text{on}}$ : pulse-on period;  $T_{\text{off}}$ : pulse-off period.

### 3.2 Characterization of Ag/TiO<sub>2</sub> nanotube array electrodes

Fig. 2a shows a typical SEM image of the Ag nanoparticles deposited on the non-porous TiO<sub>2</sub> film by anodizing in 1 M H<sub>2</sub>SO<sub>4</sub>. It can be seen that highly dispersed Ag nanoparticles with a size of 2–10 nm cover the surface. Fig. 2b–d show SEM images of Ag nanoparticles deposited on a TiO<sub>2</sub> nanotube array film (100 cycles). Similarly, the film is uniform without obvious agglomeration on the TiO<sub>2</sub> nanotube array surface. The EDX spectrum (inset of Fig. 2b) confirms the presence of Ag and shows a content of about 0.45 at%. From the high magnification images (Fig. 2c and d), the vertically oriented TiO<sub>2</sub> nanotubes, with an inner diameter of approximately 80 nm and a wall thickness of about 15 nm, were entirely covered by Ag particles. When the pulse deposition time is increased to 200 cycles (Fig. 2e and f), uniform Ag nanoparticles in a cluster form (5–12 nm) can be clearly observed on top of the tubes. Also, it is more likely that more Ag particles are deposited on the bottom of the nanotube due to the higher electric current intensity.<sup>36</sup> Direct evidence of this is provided by the TEM image in Fig. 3.

For comparison, the morphologies of Ag/TiO<sub>2</sub> nanotubes prepared by the conventional photocatalytic reduction (PR) for 5 min are shown in Fig. 4a and b. It is apparent that non-uniform Ag particles with a size variation from 20 nm to 1 μm are preferably located at the tube openings. The amount of Ag nanoparticles, estimated by the EDX measurement, is about 0.56 at%, which is comparable to that obtained by PC deposition. The average diameter of Ag particles prepared by the photocatalytic reduction method is much larger than that prepared by PC deposition. To further verify the effect of Ag particle size distribution on the photoelectrochemical performance of Ag/TiO<sub>2</sub> electrodes, we have developed an ultrasound-assisted PR technique to fabricate uniform Ag particles with a diameter of about 10–20 nm (Fig. 4c and d). The distribution of Ag particles on the TiO<sub>2</sub> nanotubes is better than that by the conventional PR technique, and the particle size is close to that prepared by PC deposition.

The chemical states of the elements in the Ag particle-coated TiO<sub>2</sub> samples were analyzed by X-ray photoelectron spectroscopy (XPS). Previous studies have shown that the

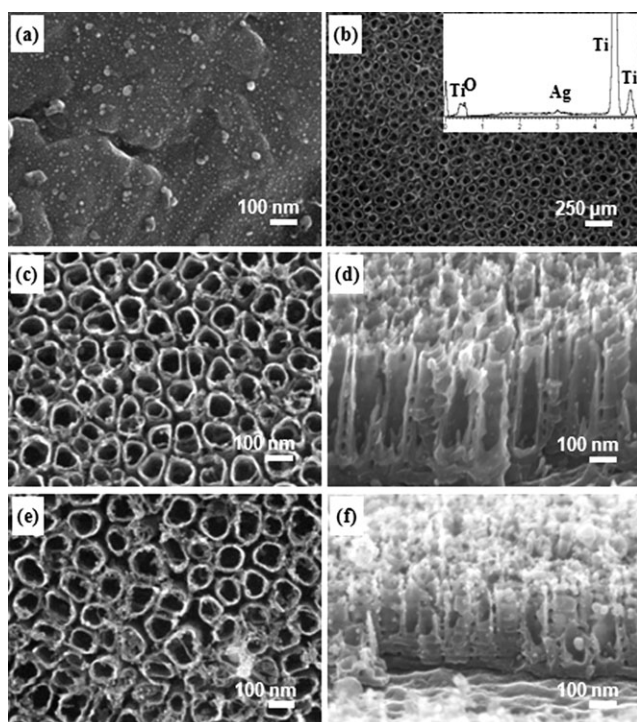


**Fig. 2** SEM images of Ag/TiO<sub>2</sub> films prepared by PC deposition: (a) PC deposition of Ag nanoparticles on a smooth TiO<sub>2</sub> surface (100 cycles), (b–d) PC deposition (100 cycles) and (e, f) PC deposition (200 cycles). The inset image of (b) shows the EDX spectrum of the corresponding Ag/TiO<sub>2</sub> nanocomposites.

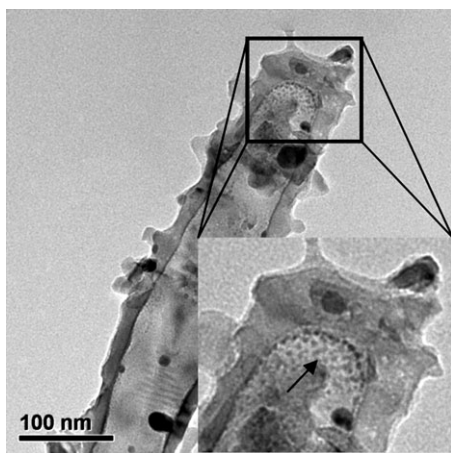


**Fig. 3** A typical TEM image of Ag particles on the TiO<sub>2</sub> nanotube wall surface.

Ag3d<sub>5/2</sub> binding energies for Ag, Ag<sub>2</sub>O and AgO are approximately 368.2, 367.8 and 367.4 eV, respectively. The survey spectrum (Fig. 5a) clearly indicates that three major sets of peaks from the O1s, Ti2p and Ag3d states exist in the Ag nanoparticle-coated TiO<sub>2</sub> nanotube sample by PC deposition. No trace of any impurity is observed, except for a small amount of adventitious carbon (C1s) from the XPS instrument itself. A high-resolution XPS spectrum confined to the Ag window (Fig. 5b) gave binding energies of Ag3d doublet peaks located at 368.5 (Ag3d<sub>5/2</sub>) and 374.5 (Ag3d<sub>3/2</sub>) eV. This reveals

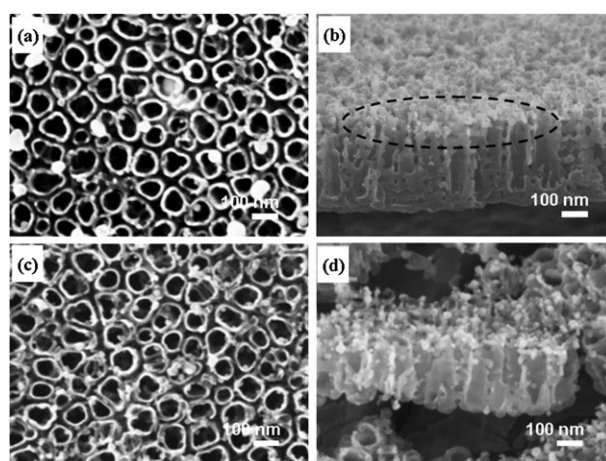
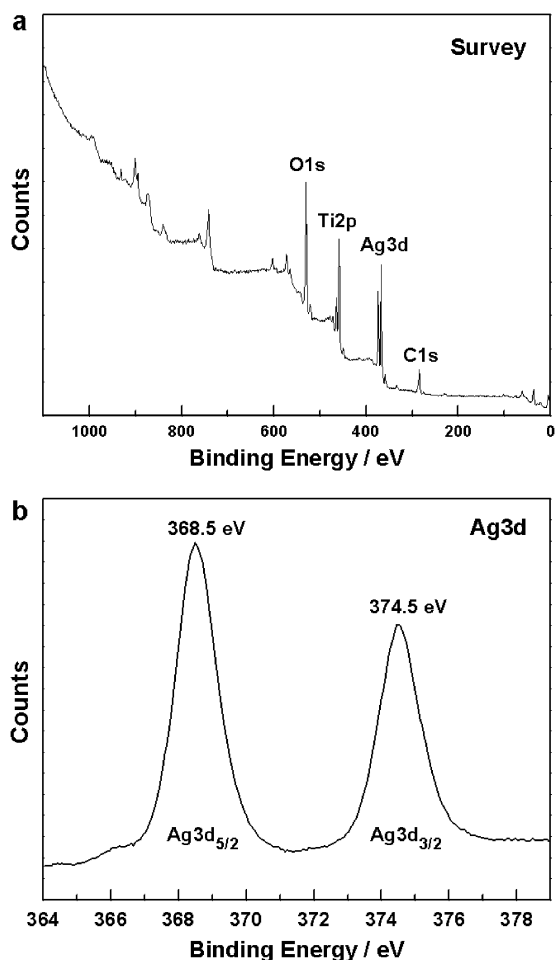


**Fig. 4** SEM images of Ag/TiO<sub>2</sub> films prepared by photocatalytic reduction deposition: (a, b) conventional photocatalytic reduction of Ag particles on TiO<sub>2</sub> nanotubes and (c, d) ultrasound-assisted photocatalytic reduction of Ag particles on TiO<sub>2</sub> nanotubes.

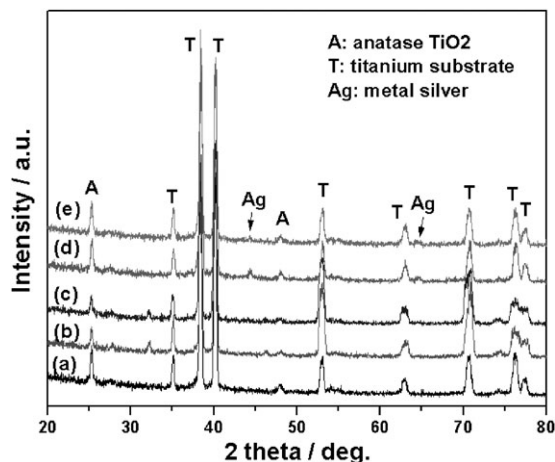
that the Ag exists in a metallic form.<sup>31,37</sup> These results are also in good agreement with the XRD characterization.

Fig. 6 shows XRD patterns of the Ag/TiO<sub>2</sub> nanotube arrays. It is clear that all the samples after 450 °C annealing show an anatase TiO<sub>2</sub> phase. The sample prepared by regular photocatalytic reduction for 5 min shows two obvious peaks corresponding to the metallic Ag (200) and (220) planes at 2θ values of about 44.3 and 64.2°, respectively (curve d). The strongest peak of Ag (111) is not visible as it might be masked by the Ti substrate peak at 2θ = 38.4°. Although they showed comparable Ag contents (~0.5 at%), there are no obvious peaks belonging to characteristic metallic Ag in the PC electrodeposition samples (curves b and c). This is due to the uniformly small and well dispersed Ag particles. The smaller Ag peaks of the Ag/TiO<sub>2</sub> sample prepared by ultrasound-assisted PR deposition verify this assumption (curve e).

The UV-vis diffuse reflection spectra of pure TiO<sub>2</sub> nanotube arrays and Ag-loaded TiO<sub>2</sub> nanotube arrays prepared by different techniques are displayed in Fig. 7. It is apparent that a small and broad absorption peak centered close to 410 nm can be found in the visible region (curve a). This phenomenon is attributed to the sub-band gap state of the special TiO<sub>2</sub> nanotube array structures.<sup>38,39</sup> The absorption edges of the samples loaded with Ag nanoparticles by PC deposition show a slight blue-shift (curves b and c). The peaks with higher intensities observed at around 360–500 nm are attributed to the surface plasmon resonance (SPR) effect of spatially confined electrons in the Ag nanoparticles.<sup>40,41</sup> It is well known that the absorption peak of Ag nanoparticles is size-dependent. An increase in the particle size red-shifts the absorption peak. Therefore, because of the synergistic effect of the coupled Ag/TiO<sub>2</sub> nanostructures, the peaks at about 390 nm in the spectra (curves b and c) indicate a very small Ag nanoparticle size by PC electrodeposition. A peak at 430 nm was recorded for the photocatalytically deposited Ag/TiO<sub>2</sub> sample (curves d and e); this implies that the size of the Ag particles prepared is larger than that by PC deposition.



**Fig. 5** XPS analysis results of the Ag/TiO<sub>2</sub> nanotube sample: (a) the survey XPS spectrum and (b) the high-resolution spectrum for the Ag 3d states.



**Fig. 6** XRD patterns of (a) 450 °C annealed TiO<sub>2</sub> nanotube sample without Ag deposition; Ag/TiO<sub>2</sub> by PC deposition for (b) 100 cycles and (c) 200 cycles; (d) Ag/TiO<sub>2</sub> by photocatalytic reduction; (e) Ag/TiO<sub>2</sub> by ultrasound-assisted photocatalytic reduction. A, T and Ag represent anatase TiO<sub>2</sub>, the titanium substrate and metallic silver, respectively.

Compared with the typical plasmon peak of Ag nanoparticles at 400 nm, the SPR band shows a large red-shift and a lower

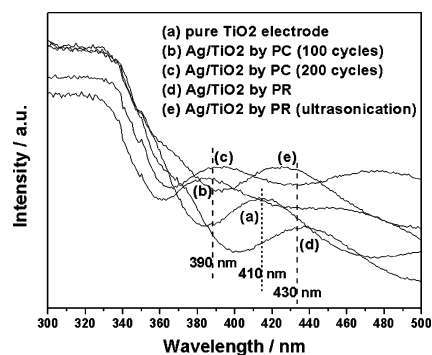


**Fig. 7** Diffuse reflection spectra of (a) a pure TiO<sub>2</sub> nanotube sample; an Ag/TiO<sub>2</sub> sample by PC deposition for (b) 100 cycles and (c) 200 cycles; an Ag/TiO<sub>2</sub> sample by (d) conventional photocatalytic reduction and (e) ultrasound-assisted photocatalytic reduction.

intensity. These SPR band shifts might be related to the interaction between Ag and TiO<sub>2</sub>.<sup>40,41</sup>

### 3.3 Photoelectrochemical properties

To compare the interfacial charge transfer resistance, electrochemical AC impedance spectra (EIS) were measured for the TiO<sub>2</sub> nanotube array films, with or without a coating of Ag nanoparticles by PC deposition. Fig. 8 shows typical Nyquist plots of EIS spectra for pure TiO<sub>2</sub> nanotube array electrodes and Ag/TiO<sub>2</sub> array electrodes, with or without UV light irradiation. The impedance arc radius of the electrodes in the dark was much bigger than that under UV light irradiation. This indicates that there were few electrons across the TiO<sub>2</sub>–electrolyte interface in the dark; while under UV light illumination, the arc radius of the Ag/TiO<sub>2</sub> nanotube array electrode is obviously smaller than that of the pure TiO<sub>2</sub> nanotube array electrode. This demonstrates that the Ag/TiO<sub>2</sub> nanotube array electrode exhibits a greater separation efficiency of photogenerated electron–hole pairs and a faster charge transfer than the pure TiO<sub>2</sub> nanotube film at the solid–liquid interface. Moreover, the Ag/TiO<sub>2</sub> electrodes by PC deposition have a superior performance to those prepared by PR deposition. These results verify that the size and distribution of Ag particles on the TiO<sub>2</sub> nanotube surface have a great effect on its photoelectrochemical performance. Therefore, the PC technique to fabricate uniform Ag nanoparticles on TiO<sub>2</sub> nanotube surfaces is a promising way to improve the efficiency of photocatalysis.

In order to examine the size-specific properties of the nanostructured Ag/TiO<sub>2</sub> hybrid materials, photocurrent spectra measurements were recorded in a photoelectrochemical measurement system. Fig. 9 shows the photocurrent vs. wavelength plots for the different TiO<sub>2</sub> nanotube array electrodes. As is shown, the coupled Ag/TiO<sub>2</sub> nanostructure exhibits a much stronger photoelectrochemical response than the pure TiO<sub>2</sub> nanotube array (~860 nA), with a peak center at around 330 nm. This peak position displays a blue-shift from the band gap of pure bulk TiO<sub>2</sub> (387 nm, 3.2 eV) due to the quantum confinement effect.<sup>42</sup> The enhanced visible light harvest is due to the more efficient electron transfer and greater surface area by the introduction of Ag nanoparticles onto the TiO<sub>2</sub>

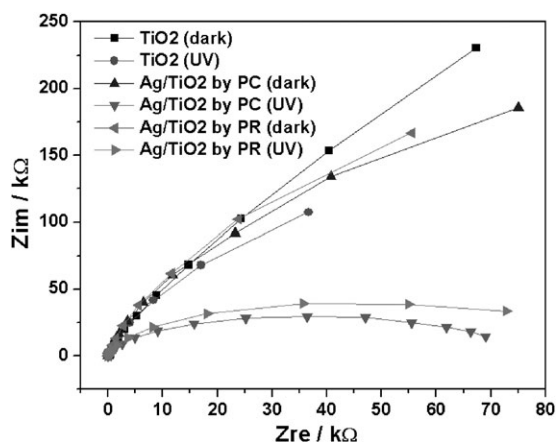


**Fig. 8** Nyquist plots of the pure TiO<sub>2</sub> nanotube array electrodes and the coupled Ag/TiO<sub>2</sub> array electrodes in the dark and under UV light illumination. PC: pulse current deposition (100 cycles); PR: photocatalytic reduction deposition.

nanotube array to form intimate Ag/TiO<sub>2</sub> heterojunctions. In the case of the three-dimensionally well-oriented Ag/TiO<sub>2</sub> coupled nanotubes prepared by the PC deposition technique (Fig. 10), the generated photocurrent is found to be greatly enhanced, with higher intensities (~1700 nA) than that of the two-dimensional, randomly distributed Ag particles prepared by regular photocatalytic reduction (~1250 nA), and also higher than that of the modified Ag/TiO<sub>2</sub> electrodes of comparable particle size fabricated by PR with the assistance of ultrasound (~1600 nA). It was also found that the photocurrent intensities of the resultant coupled Ag/TiO<sub>2</sub> nanotubes decreased with increasing deposition time. This is attributed to the smaller and more evenly sized Ag nanoparticles (“metal islands”) coated onto the TiO<sub>2</sub> nanotubes (semiconductor) that allow the formation of isolated Schottky barriers.<sup>43</sup> Schottky barriers serve as efficient electron traps to avoid electron-hole recombination. Furthermore, because of the

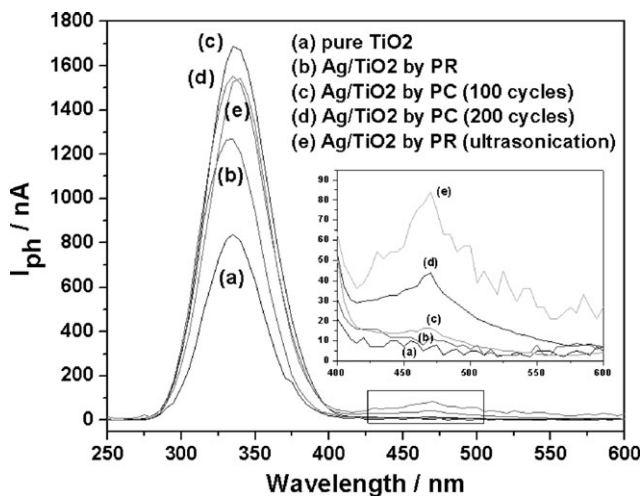


**Fig. 9** Photocurrent spectra of the pure TiO<sub>2</sub> and Ag/TiO<sub>2</sub> electrodes. The inset is the photocurrent spectra in the 400–600 nm wavelength range. PC: pulse current deposition; PR: photocatalytic reduction deposition.

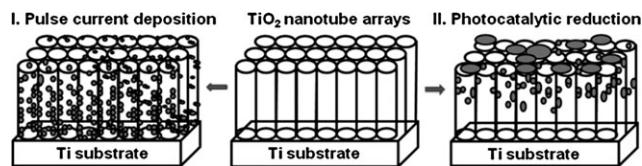


**Fig. 10** A schematic comparison of the Ag/TiO<sub>2</sub> nanotube arrays created by (I) the newly developed PC deposition technique and (II) the regular photocatalytic deposition method.

surface plasmon resonance effect of Ag, the photocurrent spectrum of the uniform coupled Ag/TiO<sub>2</sub> electrode shows a weak photocurrent response in the 410–550 nm range, with a maximum at about 470 nm (the inset of Fig. 9). However, superfluous Ag content or a large particle size distribution on the surface would block the transferring of electrons to the acceptor to some extent. These results demonstrate the necessity to optimize coupled electrode nanostructures in an orderly orientation.

The method described in this study is based on PC electrodeposition, which allows easy and controllable Ag nanoparticle dispersed deposition on titania nanotube structures. It can also be applied to produce other types of coupled metal/semiconductor nanostructures. In addition, such a versatile technique to assemble functionally coupled nanomaterials provides opportunities for improving their performance in a wide variety of other fields, such as surface-enhanced Raman scattering (SERS),<sup>44,45</sup> antibacterial biological materials,<sup>46,47</sup> photochromic devices,<sup>48–50</sup> etc.

#### 4. Conclusion

In summary, we have developed a simple pulse current electrodeposition method to fabricate small and uniform Ag nanoparticles with a narrow size distribution on TiO<sub>2</sub> nanotube array surfaces. This method effectively suppresses the rapid growth of Ag particles and promotes the uniform deposition of small Ag nanoparticles within the TiO<sub>2</sub> nanotube array, while minimizing deposition and clogging at tube entrances. The resulting electrodes contain intimately coupled three-dimensional Ag/TiO<sub>2</sub> nanostructures with greatly improved photocurrent generation and interfacial charge transfer rates compared to two-dimensional random Ag particle layers deposited directly on the upper nanotube areas by regular photoinduced deposition. This study provides a convenient way to tailor the photoelectrochemical properties of Ag/TiO<sub>2</sub> nanotube array electrodes. The same technique can also be employed for quantum dot-sensitized solar cells and photocatalysts.

#### Acknowledgements

The authors thank the National Research Foundation of Singapore Government (Grant MEWR 651/06/160), the National Nature Science Foundation of China (20773100, 20620130427), the National Basic Research Program of China (973 Program) (2007CB935603), and R&D of Fujian and Xiamen (2007H0031, 3502Z20073004).

## References

- 1 G. K. Mor, O. K. Varghese, M. Paulose, K. Shankar and C. A. Grimes, *Sol. Energy Mater. Sol. Cells*, 2006, **90**, 2011.
- 2 C. A. Grimes, *J. Mater. Chem.*, 2007, **17**, 1451.
- 3 J. M. Macak, H. Tsuchiya, A. Ghicov, K. Yasuda, R. Hahn, S. Bauer and P. Schmuki, *Curr. Opin. Solid State Mater. Sci.*, 2007, **11**, 3.
- 4 Z. Y. Liu, V. Subramania and M. Misra, *J. Phys. Chem. C*, 2009, **113**, 14028.
- 5 K. Shankar, G. K. Mor, H. E. Prakasam, S. Yoriya, M. Paulose, O. K. Varghese and C. A. Grimes, *Nanotechnology*, 2007, **18**, 065707.
- 6 H. S. Shim, S. I. Na, S. H. Nam, H. J. Ahn, H. J. Kim, D. Y. Kim and W. B. Kim, *Appl. Phys. Lett.*, 2008, **92**, 183107.
- 7 Y. K. Lai, L. Sun, Y. C. Chen, H. F. Zhuang, C. J. Lin and J. W. Chin, *J. Electrochem. Soc.*, 2006, **153**, D123.
- 8 H. F. Zhuang, C. J. Lin, Y. K. Lai, L. Sun and J. Li, *Environ. Sci. Technol.*, 2007, **41**, 4735.
- 9 J. M. Macak, M. Zlamal, J. Krysa and P. Schmuki, *Small*, 2007, **3**, 300.
- 10 M. Paulose, G. K. Mor, O. K. Varghese, K. Shankar and C. A. Grimes, *J. Photochem. Photobiol., A*, 2006, **178**, 8.
- 11 G. K. Mor, K. Shankar, M. Paulose, O. K. Varghese and C. A. Grimes, *Nano Lett.*, 2005, **5**, 191.
- 12 Y. K. Lai, X. F. Gao, H. F. Zhuang, J. Y. Huang, C. J. Lin and L. Jiang, *Adv. Mater.*, 2009, **21**, 3799.
- 13 Y. K. Lai, C. J. Lin, J. Y. Huang, H. F. Zhuang, L. Sun and T. Nguyen, *Langmuir*, 2008, **24**, 3867.
- 14 O. K. Varghese, D. W. Gong, M. Paulose, K. G. Ong, E. C. Dickey and C. A. Grimes, *Adv. Mater.*, 2003, **15**, 624.
- 15 O. K. Varghese, G. K. Mor, C. A. Grimes, M. Paulose and N. Mukherjee, *J. Nanosci. Nanotechnol.*, 2004, **4**, 733.
- 16 S. H. Oh, R. R. Finones, C. Daraio, L. H. Chen and S. H. Jin, *Biomaterials*, 2005, **26**, 4938.
- 17 Y. K. Lai, Y. X. Huang, H. Wang, J. Y. Huang, Z. Chen and C. J. Lin, *Colloids Surf., B*, 2010, **76**, 117.
- 18 Y. A. Cao, W. S. Yang, H. F. Zhuang, G. Z. Liu and P. Yue, *New J. Chem.*, 2004, **28**, 218.
- 19 J. G. Yu, Q. J. Xiang and M. H. Zhou, *Appl. Catal., B*, 2009, **90**, 595.
- 20 R. Asahi, T. Monkawa, T. Ohwaki, K. Aoki and Y. Taga, *Science*, 2001, **293**, 269.
- 21 M. H. Zhou and J. G. Yu, *J. Hazard. Mater.*, 2008, **152**, 1229.
- 22 C. X. Feng, Y. Wang, Z. S. Jin, J. W. Zhang, S. L. Zhang, Z. S. Wu and Z. J. Zhang, *New J. Chem.*, 2008, **32**, 1038.
- 23 C. L. Wang, L. Sun, H. Yun, J. Li, Y. K. Lai and C. J. Lin, *Nanotechnology*, 2009, **20**, 295601.
- 24 Y. K. Lai, Z. Q. Lin, J. Y. Huang, L. Sun, Z. Chen and C. J. Lin, *New J. Chem.*, 2010, **34**, 44.
- 25 A. Benoit, I. Paramasivam, Y. C. Nah, P. Roy and P. Schmuki, *Electrochem. Commun.*, 2009, **11**, 728.
- 26 L. X. Yang, D. M. He, Q. Y. Cai and C. A. Grimes, *J. Phys. Chem. C*, 2007, **111**, 8214.
- 27 J. M. Macak, F. Schmidt-Stein and P. Schmuki, *Electrochem. Commun.*, 2007, **9**, 1783.
- 28 I. Paramasivam, J. M. Macak and P. Schmuki, *Electrochem. Commun.*, 2008, **10**, 71.
- 29 D. Kannaiyan, M. A. Cha, Y. H. Jang, B. H. Sohn, J. Huh, C. Park and D. H. Kim, *New J. Chem.*, 2009, **33**, 2431.
- 30 Y. K. Lai, Y. C. Chen, H. F. Zhuang and C. J. Lin, *Mater. Lett.*, 2008, **62**, 3688.
- 31 J. A. Toledo-Antonio, M. A. Cortes-Jacome, C. Angeles-Chavez, E. Lopez-Salinas and P. Quintana, *Langmuir*, 2009, **25**, 10195.
- 32 Y. K. Lai, C. J. Lin, H. Wang, J. Y. Huang, H. F. Zhuang and L. Sun, *Electrochem. Commun.*, 2008, **10**, 387.
- 33 Y. K. Lai, H. F. Zhuang, L. Sun, Z. Chen and C. J. Lin, *Electrochim. Acta*, 2009, **54**, 6536.
- 34 S. S. Kim, S. I. Na, J. Jo, D. Y. Kim and Y. C. Nah, *Appl. Phys. Lett.*, 2008, **93**, 073307.
- 35 S. S. Kim, Y. C. Nah, Y. Y. Noh, J. Jo and D. Y. Kim, *Electrochim. Acta*, 2006, **51**, 3814.
- 36 D. Gong, C. A. Grimes, O. K. Varghese, W. C. Hu, R. S. Singh, Z. Chen and E. C. Dickey, *J. Mater. Res.*, 2001, **16**, 3331.
- 37 G. I. N. Waterhouse, G. A. Bowmaker and J. B. Metson, *Appl. Surf. Sci.*, 2001, **183**, 191.
- 38 D. W. Bahnemann, R. Dillert and P. K. J. Robertson, *Chemical Physics of Nanostructured Semiconductors*, XSP BV, Eindhoven, 2003.
- 39 Y. K. Lai, L. Sun, C. Chen, C. G. Nie, J. Zuo and C. J. Lin, *Appl. Surf. Sci.*, 2005, **252**, 1101.
- 40 H. J. Zhang, X. Y. Li and G. H. Chen, *J. Mater. Chem.*, 2009, **19**, 8223.
- 41 J. He, I. Ichinose, T. Kunitake and A. Nakao, *Langmuir*, 2002, **18**, 10005.
- 42 G. Wang, Q. Wang, W. Lu and J. H. Li, *J. Phys. Chem. B*, 2006, **110**, 22029.
- 43 Z. C. Shan, J. J. Wu, F. F. Xu, F. Q. Huang and H. M. Ding, *J. Phys. Chem. C*, 2008, **112**, 15423.
- 44 A. Roguska, A. Kudelski, M. Pisarek, M. Lewandowska, K. J. Kurzydowski and M. Janik-Czachor, *Surf. Sci.*, 2009, **603**, 2820.
- 45 A. Roguska, A. Kudelski, M. Pisarek, M. Lewandowska, M. Dolata and M. Janik-Czachor, *J. Raman Spectrosc.*, 2009, **40**, 1652.
- 46 W. Su, S. S. Wei, S. Q. Hu and J. X. Tang, *J. Hazard. Mater.*, 2009, **172**, 716.
- 47 H. J. Zhang and G. H. Chen, *Environ. Sci. Technol.*, 2009, **43**, 2905.
- 48 I. Paramasivam, J. M. Macak, A. Ghicov and P. Schmuki, *Chem. Phys. Lett.*, 2007, **445**, 233.
- 49 K. Matsubara and T. Tatsuma, *Adv. Mater.*, 2007, **19**, 2802.
- 50 Y. C. Nah, S. S. Kim, J. H. Park, H. J. Park, J. Jo and D. Y. Kim, *Electrochem. Commun.*, 2007, **9**, 1542.